Oxygen incorporated during deposition determines the crystallinity of magnetron-sputtered Ta3N5 films

M. Rudolph, I. Vickridge, E. Foy, J. Alvarez, Jean-Paul Kleider, D. Stanescu, H. Magnan, N. Herlin-Boime, B. Bouchet-Fabre, T. Minea, et al.

Oxygen incorporated during film growth determines the crystallinity of magnetron-sputtered Ta_3N_5 films

M. Rudolph[1,6], I. Vickridge[2], E. Foy[3], J. Alvarez[4], J.-P. Kleider[4], D. Stanescu[5], H. Magnan[5], N. Herlin-Boime[6], B. Bouchet-Fabre[6], T. Minea[1], M.-C. Hugon[1]

[1] LPGP, UMR 8578 CNRS, Université Paris-Sud, Université Paris-Saclay, 91405 Orsay, France

[2] INSP, Sorbonne Université, Université Pierre et Marie Curie, 75005 Paris

[3] LAPA-IRAMAT, NIMBE, CEA, CNRS, Université Paris-Saclay, CEA Saclay, 91191 Gif-sur-Yvette, France

[4] GeePs, CNRS UMR8507, CentraleSupelec, Univ Paris-Sud, Université Paris-Saclay, Sorbonne Université, 91192 Gif-sur-Yvette, France

[5] SPEC, CEA/CNRS, Université Paris-Saclay, 91191 Gif-sur-Yvette, France

[6] NIMBE, CEA/CNRS, Université Paris-Saclay, 91191 Gif-sur-Yvette, France

Abstract

Ta_3N_5 belongs to the group of transition metal nitrides with the cation in a high formal oxidation state. These are, in general, difficult to synthesize owing to the low reactivity of nitrogen. This applies similarly to Ta_3N_5 that crystallizes only in the presence of oxygen during synthesis. Typical preparation methods are ammonolysis of oxidized Ta or magnetron sputtering of a Ta target in an atmosphere of Ar, N_2 and O_2. However, the thin films typically obtained by either synthesis method are of varying degree of crystallinity and the parameters affecting the crystallinity remain unclear. In this study, we identify oxygen to be the central driver for the crystallinity of Ta_3N_5 thin films prepared by magnetron sputtering. While little oxygen in the films yields the metallic δ-TaN phase, excess oxygen results in low crystallinity Ta_3N_5 or amorphous Ta-O-N films. Ta_3N_5 samples with a high degree of crystallinity are obtained by

limiting the oxygen supply to the sample during the deposition. Comparison with other studies suggest a fundamental oxygen incorporation limit above which the crystallinity of Ta_3N_5 is compromised. The most crystalline sample from this study contains 4.4 at.% of oxygen. It is grown onto a Si(100) substrate, covered with a 30 nm-thick metallic Ta layer. Large Ta_3N_5 grains between 80 and 120 nm in size are obtained.

1 Introduction

Ta_3N_5 is a promising candidate as a photon absorber in solar water splitting devices because its valence and conduction bands straddle the oxygen and hydrogen evolution potentials [1]. At the same time, it can absorb a large part of the solar spectrum owing to its small band gap of 2.1 eV [1, 2]. In fact, it is very close to the assumed optimum band gap of around 2.0 eV, which is the compromise between the fraction of absorbed sunlight and the electric potential necessary to split water into oxygen and hydrogen [3]. One important parameter for the Ta_3N_5 photon absorber regarding the application in view is a high degree of crystallinity. This is because non-crystalline regions, in form of grain boundaries or amorphous content, represent sites of recombination for photogenerated charge carriers, reducing the overall device efficiency. However, Ta_3N_5 thin films prepared so far by ammonolysis or magnetron sputtering show varying degrees of crystallinity and the central parameter to control the crystallinity remains yet unclear.

The formation of Ta_3N_5 is triggered by oxygen incorporation [4,5,6]. This applies to both principal preparation routes, ammonolysis and magnetron sputtering. Ammonolysis typically requires an oxidized tantalum precursor that is annealed under a flow of NH_3. In this process, nitrogen diffuses into the material and partially replaces the oxygen anions in the lattice [7]. The process requires high temperatures (> 680° C) and can take up to several hours [8,9,10]. In general, the sample crystallinity increases with the thermal budget [9]. Grain sizes obtained by this method are a few 10s of nm only, though. E.g., Pinaud *et al.* [8] measure average grain

sizes between 17.3 nm and 17.7 nm and Dabirian *et al.* [9] observe average grain sizes between 22 nm and 36 nm.

Magnetron sputtering of a Ta target in a gas mixture of Ar, N_2 and O_2 is an alternative synthesis route. It offers a reduced thermal budget compared to ammonolysis with crystalline samples obtained at substrate temperatures between 400° and 600° C [11]. However, magnetron sputtering at these temperatures often results in a low degree of crystallinity [5,6]. Crystallinity improves by increasing the substrate temperature to values close to those necessary for ammonolysis. Ishihara *et al.* achieve a higher degree of crystallinity of their magnetron-sputtered Ta_3N_5 thin films by using a higher substrate temperature, i.e. 800° C, compared to the onset temperature for crystallization found between 400° to 600° C [11]. Alternatively, annealing sputtered Ta_3N_5 samples in NH_3 at 750° C for 15h after the deposition is similarly successful in improving the sample crystallinity [5].

The studies listed above suggest a strong effect of the thermal budget on the crystallinity of Ta_3N_5 thin films, though its direct effect on the crystallinity is not conclusively proven. Possible may also be an indirect correlation and we suggest the oxygen content in the film to link the thermal budget with the crystallinity. We therefore focus our investigation on the isolated effect of oxygen on the crystallinity of the samples. This is possible by magnetron sputtering, as the oxygen incorporation can be tuned during the sputtering process while leaving all other process parameters, in particular the thermal budget, constant. The oxygen content, calculated as the ratio O/(Ta+N+O) and expressed in at.%, is quantified using Rutherford backscattering spectrometry (RBS) and nuclear reaction analysis (NRA). The obtained sample composition is then correlated with the crystalline structure from grazing-incidence X-ray diffraction (GI-XRD). To support the results from GI-XRD, the surface is imaged by atomic force microscopy (AFM) and scanning electron microscopy (SEM). Finally, two samples having different oxygen content are used to measure the photocurrent in an electrochemical cell under illumination.

2 Film preparation and characterization techniques

The films were prepared by ion-assisted growth using a balanced magnetron with two external magnetic coils to increase the ion flux onto the substrate [12]. Measurements of the ion saturation current together with the area density measurements from the ion beam analysis (see below) revealed an ion-to-neutral flux ratio of 0.3 in standard balanced magnetron configuration and 2.8 using the external magnetic coils. The magnetron was installed in a vacuum chamber with a base pressure of $< 5 \cdot 10^{-4}$ Pa. The Ta target was of 99.95% purity and had a diameter of 10 cm. The power applied to the cathode was 80 W corresponding to a cathode potential of -330 V. The cathode potential was intentionally kept small in order to limit the rate of high energy (> 100 eV) Ar neutrals backscattered from the target, that risked to incorporate defects into the growing film [13].

The films were deposited on polished monocrystalline Si(100) and Ta foil substrates. Films on the Si substrate were used to determine their structure, elemental composition, crystallinity and topography. Films on the Ta foil substrate were used to test their photoactivity in a photoelectrochemical cell.

Prior to deposition, the substrates were cleaned in a bath of isopropanol for 5 min and then blown dry with N_2. They were then clamped onto a substrate holder and inserted into the deposition chamber. The substrates were sputter-etched for 10 min at an effective DC bias of -100 V by Ar ions from a radio-frequency plasma. At the same time, with a closed shutter in front of the magnetron, the target was sputter-etched at 80 W in DC mode for 10 min in pure Ar. Afterwards, the surface was conditioned by sputtering for further 10 min but using the gas composition of the following deposition.

The samples were deposited at a pressure of 0.5 Pa. The N_2 flowrate was 20 sccm, the O_2 flowrate was varied between 0.0 sccm and 0.9 sccm and Ar was added to reach a total flowrate of 50 sccm. The substrate temperature during deposition was kept constant at 600° C. Before

the deposition, a 30 nm-thick metallic Ta interlayer was deposited at room temperature onto the substrates in order to provide the same growth conditions for the Ta_3N_5 film on both types of substrates. It is important to note that this layer had a considerable effect on the crystallinity of the Ta_3N_5 phase as discussed below. Each Ta_3N_5 thin film was deposited to obtain a 250 nm-thick layer which took around 30 min. The thickness was confirmed by using a mechanical profilometer on the edge of a region shadowed during the deposition.

The composition of the samples was measured using ion beam analysis with the SAFIR platform of Sorbonne Université. The ^{181}Ta area density (AD) was determined using RBS at an α beam energy of 2000 keV. The AD of the underlying 30 nm-thick Ta layer was measured on a separate substrate and subtracted for the determination of the film composition. Minor levels of Ar were found in the films by RBS (≈ 1 at.%), which were neglected for the analysis presented here. The nitrogen and oxygen AD were determined by NRA using the nuclear reactions $^{14}N(d,\alpha)^{12}C$ at 1400 keV and $^{16}O(d,p)^{17}O$ at 850 keV.

The crystalline structure was determined by GI-XRD using a custom-built setup. It consisted of a 30 µm × 50 µm thick X-ray beam from a Mo anode (λ_{alpha} = 0.071 nm) that was incident on the sample at 0.5° to the sample surface. Diffracted rays were recorded using a photo-sensitive plate that was digitized using a scanner. The software fit2d [14] was used to integrate the spherical diffraction patterns resulting in the diffractograms presented here. The background was intentionally not subtracted.

The photocurrent was measured in a custom-built photoelectrochemical cell in a three-electrode configuration [15]. The sample was mounted as the working electrode, a Pt wire as a counter electrode and an Ag/AgCl/sat. KCl as a reference electrode. The electrolyte was an aqueous solution with 0.1 M K_2SO_4 and KOH added to obtain a pH of 13. Potential control and current acquisition were done using a Princeton Applied Research 263A potentiostat. For photocurrent−voltage curves, the potential was swept from −0.4 to +0.4 V *vs.* Ag/AgCl/sat. KCl

with a rate of 50 mV/s. The sample was illuminated through a quartz window by intermittent light from a Newport Xe arc lamp. It was equipped with an infrared filter to prevent the sample from heating up. The irradiance at the sample position was 21 mW/cm^2.

3 Thin film characterization

3.1 Elemental composition and crystallinity

The composition of the films is presented in Fig. 1 as a function of the O_2 flowrate injected into the reactor during the sputtering process. At 0 sccm O_2, the thin film is saturated with nitrogen. The sample contains 37.6 at.% of tantalum, 60.9 at.% of nitrogen and a small amount of oxygen. Similar results are obtained by Sun *et al.* [16] for magnetron-sputtered Ta-N, who find an increasing nitrogen content with increasing the N_2 supply to the reactor. This trend continues until the nitrogen incorporation saturates at around 60 at.% of nitrogen, a value very similar to the 60.9 at.% found in our experiments. Stoichiometric Ta_3N_5, in comparison, contains 62.5 at.% of nitrogen, which is slightly higher.

The reason for the lower nitrogen content measured in our sample, compared to the ideal composition of Ta_3N_5, can be explained by a small amount of oxygen incorporated. This originates from the background O_2 present in the deposition chamber even without intentionally injecting O_2 via the flowmeters. During deposition, this oxygen is preferentially incorporated due to its lower free energy of formation [17]. Once incorporated, it prevents further uptake of nitrogen to keep the charge balance between the anions and the Ta cation.

At an O_2 flowrate between 0.1 and 0.6 sccm, the oxygen incorporated into the film increases linearly. This indicates that the magnetron target is not yet in its poisoned state with respect to oxygen, so that all O_2 supplied to the process chamber is immediately gettered by sputtered Ta [6]. The linear correlation is left between 0.6 sccm and 0.7 sccm O_2 from which point on, high

levels of oxygen are incorporated into the film, due to a reduced Ta deposition rate from a poisoned target [18].

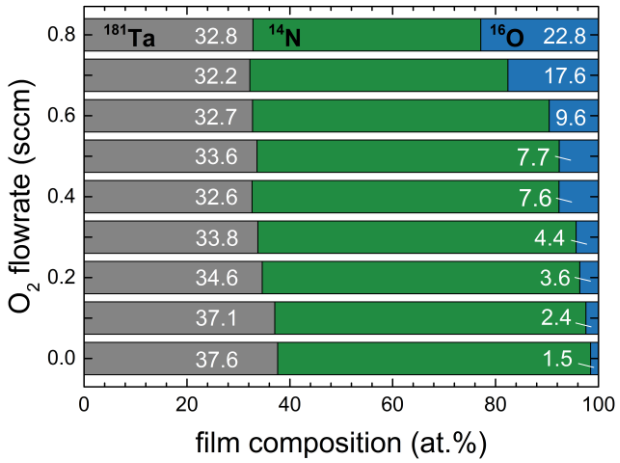

Fig. 1: Elemental composition of samples prepared at varying O_2 flowrates.

The crystallinity of the deposited films is measured on the same samples as those used to determine the elemental composition. Without any intentional oxygen supplied to the reactor during deposition (0 sccm O_2), the metallic δ-TaN phase is obtained (Fig. 2). By increasing the oxygen supply to 0.1 and 0.2 sccm O_2, a phase mixture between δ-TaN and Ta_3N_5 appears. Only at an O_2 flow of 0.3 sccm, corresponding to an oxygen content of 4.4 at.% in the film, the diffractogram shows a single phase Ta_3N_5 signature . The peaks match that of the orthorhombic Ta_3N_5 structure (powder diffraction file 01-079-1533 from the International Centre for Diffraction Data (ICDD) database). Note, that with the diffractometer used, we cannot distinguish between the monoclinic [19] and the orthorhombic [20,21] Ta_3N_5 structure because both have similar peak positions.

Increasing the O_2 supply deteriorates the crystallinity of the sample. At 0.5 sccm of O_2, the diffractogram exhibits lower peak intensities. At even higher flowrates, the peaks vanish completely. The sample deposited at 0.7 sccm O_2 exhibits two broad halos around 23 nm^{-1} and 44 nm^{-1} instead. This indicates a Ta-O-N thin film with a lack of long-range order. The observed

halos are similarly found by other authors studying Ta-O-N thin films [12,22,23] and can be attributed to some remaining local order.

The samples presented above all have a 30 nm-thick Ta interlayer between the Si substrate and the Ta_3N_5 thin film. This has a crucial influence on the crystallinity, which is illustrated by depositing a film directly onto a Si(100) substrate. While the reference sample with a Ta interlayer shows sharp diffraction peaks in GI-XRD experiments, the diffractogram of the sample missing the Ta interlayer exhibits no peaks at all proving the lack of crystallinity (Fig. 3). Possible explanations for this could be that the Ta interlayer represents a nucleation layer for Ta_3N_5. Another possibility is that Si impurities in Ta-O-N prevent its crystallization to Ta_3N_5. Si-Ta alloy formation is observed at temperatures of 700° C [24], close to the 600° C substrate temperature used in this study. A Ta interlayer could therefore act as a diffusion barrier, keeping Si out of the Ta_3N_5 film. Similarly to our experiments, de Respinis *et al.* [25] sputtered on top of their fused silica substrate a 5 nm-thick layer of Ti, before depositing metallic Ta that was subsequently oxidized and nitrided to form Ta_3N_5. They mention the possibility that the Ti interlayer may affect the crystallization behavior of Ta_3N_5 without giving further details. The Ti interlayer in their case could therefore similarly act as a diffusion barrier against the Si that is present in their fused silica substrate.

3.2 Morphology and surface topography

Two selected samples deposited at 0.3 and 0.5 sccm O_2 are imaged by SEM (Fig. 4). The surface of the first one is densely covered by crystallites with diameters between 80 nm and 120 nm. As no other phase as Ta_3N_5 is detected in the diffractograms (Fig. 2), the crystallites likely have the Ta_3N_5 structure. In between crystallites, the image shows some featureless areas that we assign to small amounts of an amorphous matrix, indicating that further fine-tuning of the oxygen content in the films may be possible. The cleaved cross-section of the sample shows a columnar-grown film. The cross-section appears rough, suggesting the presence of crystallites

throughout the film thickness. On the other hand, the sample deposited at a higher O_2 flowrate (0.5 sccm) shows a reduced density of crystallites. The crystallites also appear less pronounced and their boundaries vanish in a dominating featureless matrix. Similarly, the cleaved cross-section is flat and without perceivable texture compared to the sample deposited at a lower O_2 flowrate. The loss of crystallinity at higher O_2 flowrates seen in the SEM images matches well with the trend observed in the diffractograms.

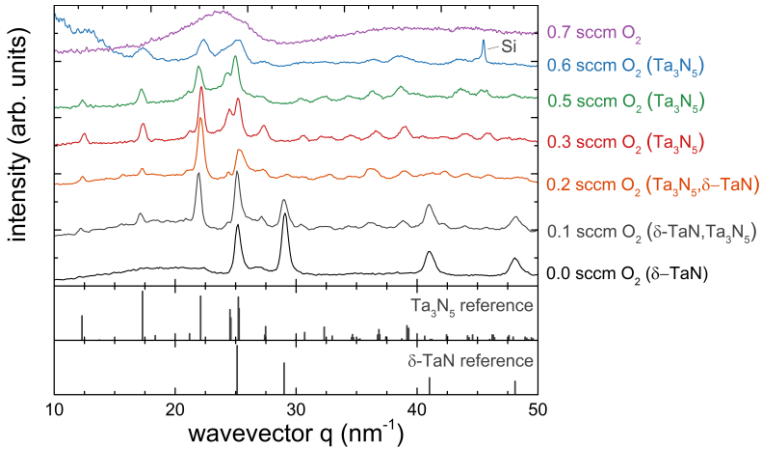

Fig. 2: GI-XRD diffractograms as a function of O_2 flowrate supplied during the deposition. The reference is taken from the powder diffraction file 01-079-1533 (Ta_3N_5) and 01-089-5196 (δ-TaN) in the ICDD database. The narrow peak on the sample deposited at a flow of 0.6 sccm O_2 stems from the underlying Si substrate.

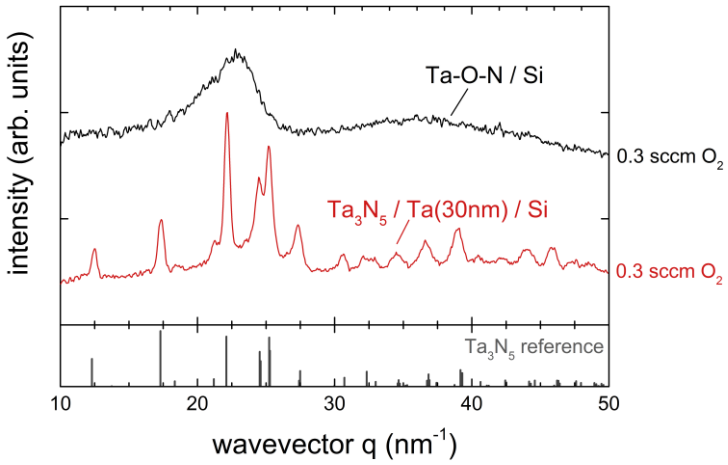

Fig. 3: Influence of a 30 nm-thick Ta interlayer on the crystallinity of the Ta_3N_5 thin films deposited at 0.3 sccm O_2.

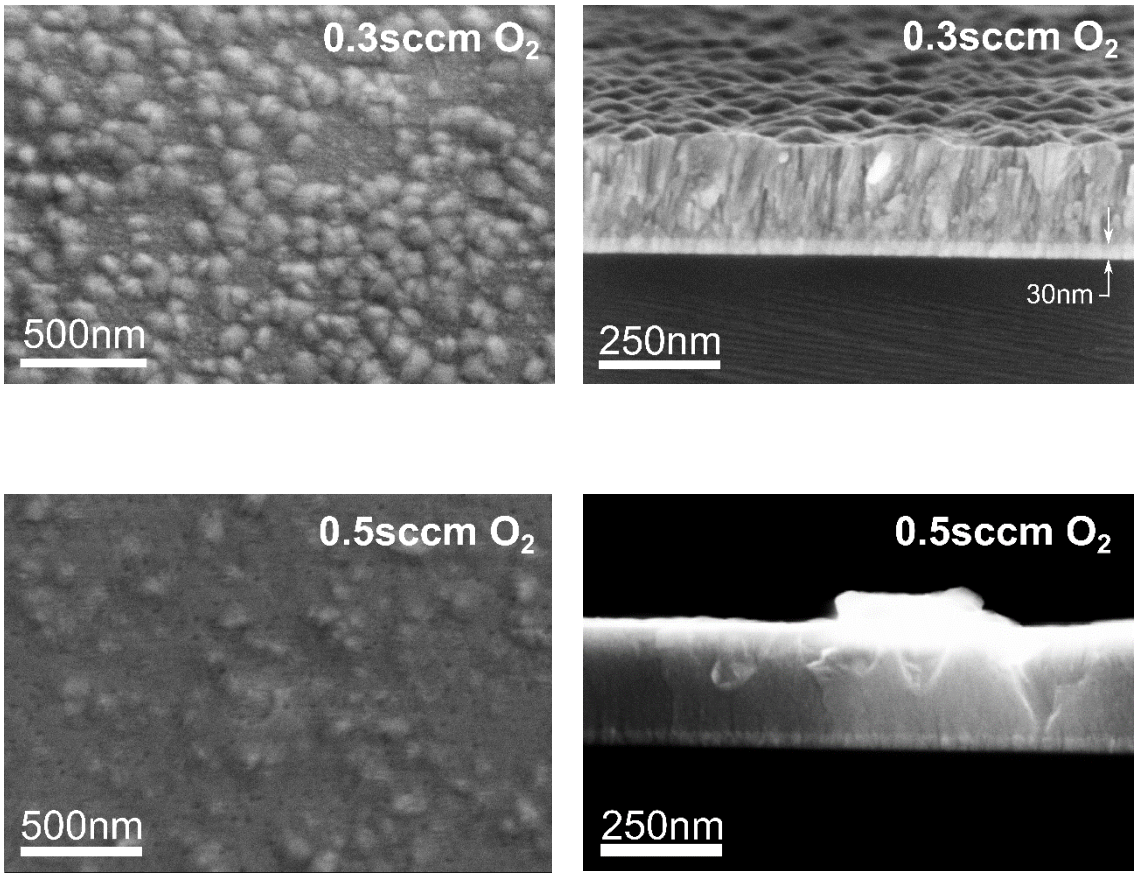

Fig. 4: Scanning electron microscopy images of the sample deposited at O_2 flowrates of 0.3 sccm (top) and at 0.5 sccm (bottom), respectively. The cross-section images on the left exhibit the 30 nm-thick Ta interlayer.

AFM images reveal the topography of the surface (Fig. 5). At a low O_2 flowrate (0.2 sccm), the surface is rough. While the highest point lies 63 nm above the baseline, most of the surface lies between 0 and about 30 nm. The comparison with the SEM images suggests, that this roughness is due to crystallites peeking out of the surface. As this sample has a dominating Ta_3N_5 signature according to its diffractogram, we suggest that these are mainly Ta_3N_5 crystallites. Increasing the O_2 flowrate decreases the roughness, in line with the observation from the SEM images, that when crystallinity is lost, the surface becomes increasingly flat due to a dominating amorphous content. At the highest O_2 flowrate of 0.7 sccm, the sample becomes completely flat with the highest point at only 3 nm above the baseline. This is in line with the observation from GI-XRD, *i.e.* the sample is nanocrystalline or amorphous.

The sample deposited at a flowrate of 0.6 sccm still contains some Ta_3N_5 crystallites, according to its diffractogram (Fig. 2). The AFM image, however, shows a flat surface covered with what appears as dips or holes. This sample with its high content of oxygen (9.6 at.%) is at the border of a vanishing Ta_3N_5 structure. The surface may therefore easily be changed by a small amount of extra oxygen. This is likely supplied at the end of the deposition process. When the magnetron is switched off, the deposition of fresh Ta onto the growing film and the reactor walls stops and so does the gettering of oxygen from the gas phase on these surfaces. At this moment, the oxygen concentration in the reactor rises during a short period of an estimated few tens of seconds, while the sample is still at an elevated temperature. The surface can therefore continue to oxidize causing the surface structure to collapse. This supports the conclusion from above that the Ta_3N_5 structure cannot tolerate excessive amounts of oxygen.

The experiments presented here show a wide range of degrees of crystallinities of Ta_3N_5 thin films. It is important to note that each film is deposited with the same thermal budget during the sputtering process and by adjusting only the O_2 flowrate and with that, the oxygen content in the film. The conclusion from these experiments is therefore that the crystallinity of

magnetron-sputtered Ta_3N_5 thin films is determined by the oxygen incorporation into the film, which can be tuned by the oxygen supplied during the sputtering process.

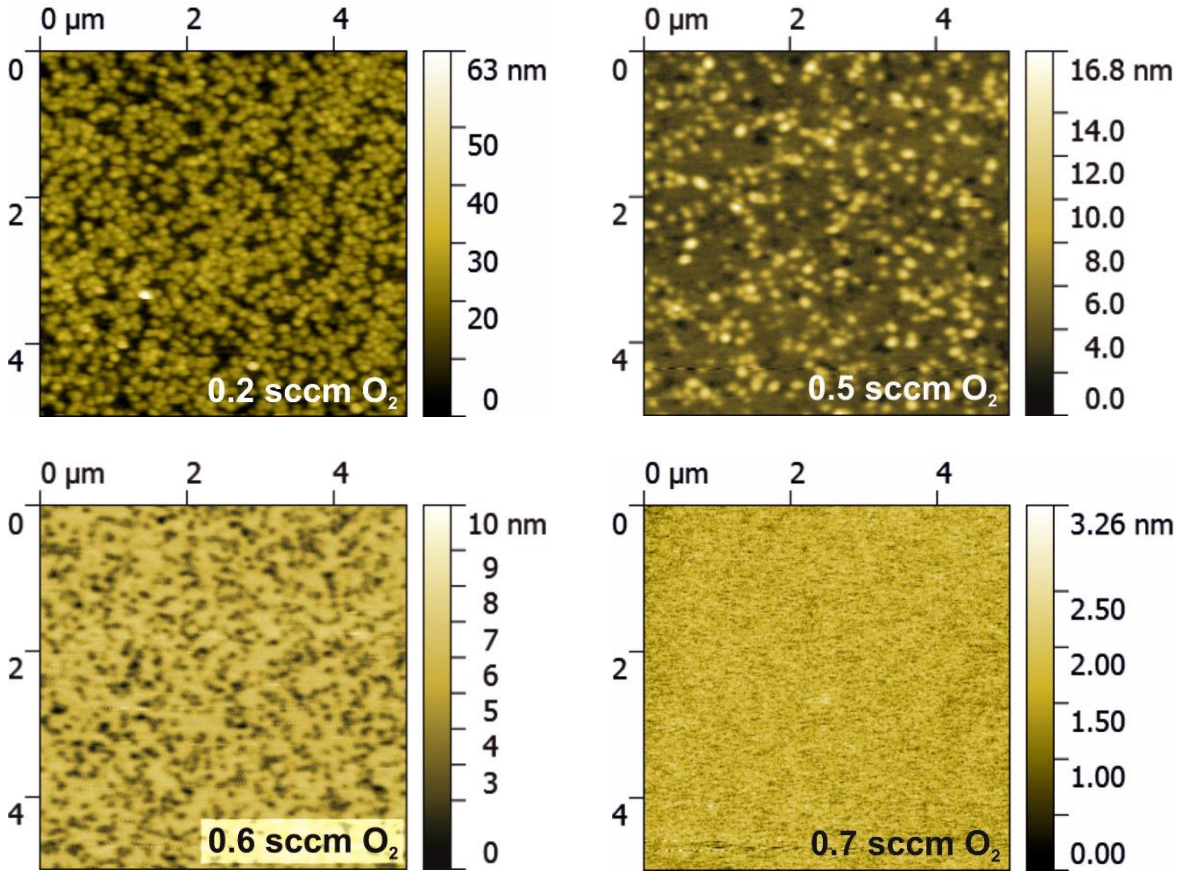

Fig. 5: Surface topology measured by AFM as a function of O_2 flowrate. Note the different height scales on the right of each image.

3.3 Photocurrent measurements

Photocurrent measurements in a photoelectrochemical cell under intermittent light prove the photoactivity of the deposited Ta_3N_5 films (Fig. 6). The experiments are done with two samples deposited at 0.3 sccm and 0.5 sccm O_2 flowrate, thus containing 4.4 at.% and 7.7 at.% of oxygen, respectively. According to their diffractograms and SEM images, these are representative samples for a Ta_3N_5-crystalline film and a Ta_3N_5 film having a low crystallinity.

The photoactivity of these samples is evaluated in five consecutive scans. For both samples, the photocurrent decreases strongly with each repetition of the experiment. This is due to a self-oxidation of the surface by photogenerated holes as suggested by Ishikawa *et al.* [26]. He *et al.* [27] show that the oxidation is self-limiting and restricted to a few nm. However, the thin oxide pins the Fermi levels at the surface, reducing the band bending. As a consequence, charge carrier separation becomes successively less efficient. Finally, the photocurrent practically ceases. In this state, the surface is limiting the photocurrent and the enhanced bulk properties of the sample containing more oxygen do not make a difference any more. Mitigation methods aim to separate the Ta_3N_5 photoabsorber from the electrolyte which in some cases can also accelerate the hole transfer from the photoanode to the electrolyte [5,9,27,28]. These layers are not further investigated here.

Comparing the first photocurrent-voltage curves obtained with each sample, the high crystallinity sample (deposited at 0.3 sccm O_2) shows a lower photocurrent than the low crystallinity one (deposited at 0.5 sccm O_2). The latter contains more oxygen, which is known to widen the band gap [6,29,30]. Therefore, on the one hand, it can be expected to absorb less photons of the light spectrum which would result in a lower density of photogenerated charge carriers. On the other hand, the larger band gap could induce a higher open circuit voltage promoting the charge carrier transfer to the electrolyte. The higher photocurrent for the oxygen-rich sample suggests that latter effect dominates here.

Nevertheless, our observation is in discrepancy with other authors that observe the inverse effect. Yokohama *et al.* [5] increase the initial low crystallinity of their sputtered samples in the as-processed state by annealing them in NH_3. They observe a strong increase in photocurrent after this treatment and assign it to the improved crystallinity. Li *et al.* [31] prepare their Ta_3N_5 nanorods by ammonolysis. They improve the photoactivity of their sample by annealing it at

1000° C instead of 850° C, which they attribute partially to an improved interface between the semiconductor and the substrate, and partially to a higher crystallinity.

Our observation that the sample deposited at 0.5 sccm O_2 shows a higher photocurrent can be understood by assuming that both samples still contain a high density of defects that acts as sites of carrier recombination. Such a material would have a small minority carrier diffusion length, i.e. the contribution to the photocurrent from minority carriers originating from the bulk is reduced. In this case, the photocurrent would arise from the surface of the photoanode where carriers are immediately separated by the electric field in the space charge layer and thus escape recombination. In this case, a slightly larger band gap caused by a higher oxygen content in the film deposited at 0.5 sccm O_2 would not be detrimental as the surface would be sensitive in particular to UV and blue light. The higher initial photocurrent of this sample could then be attributed to a higher open circuit voltage that results in a more efficient hole transfer to the electrolyte.

The origin of the defects in the Ta_3N_5 thin film could be the sputtering process that is known to induce material defects from the bombardment of energetic particles. These can be negative ions, e.g. O^-, that are accelerated in the plasma sheath above the cathode [32] or neutrals backscattered from the cathode [13]. An annealing treatment could help to reduce the defect density in the bulk. Note that such a treatment would be different in temperature and duration from the NH_3 annealing done by other authors to prepare Ta_3N_5 samples, as the purpose is not to improve crystallinity, but to anneal defects.

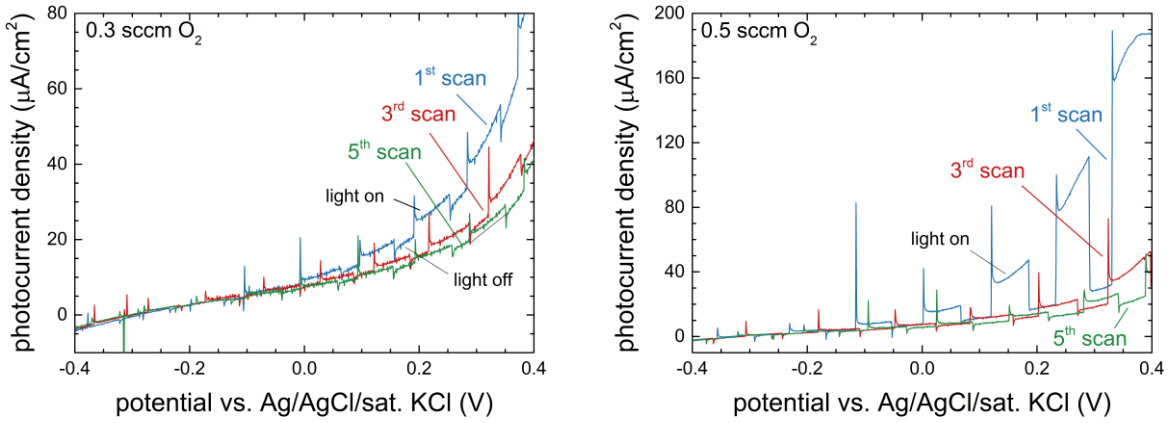

Fig. 6: On-Off photocurrent curves for two selected samples deposited at 0.3 sccm and 0.5 sccm O_2 flowrate.

3 Discussion

The study identifies oxygen being the main driver for the degree of crystallinity of magnetron-sputtered Ta_3N_5 thin films. Henderson *et al.* [10] report on the crystallinity of Ta_3N_5 samples prepared by ammonolysis. By varying temperature and duration of the process, they find that crystallinity is lost by increasing the oxygen content of their samples, similar to the results of this study. Their sample with the highest crystallinity contains 2.9 at.% of oxygen, which is in the same order of magnitude as the 4.4 at.% of oxygen found in our most crystalline sample. The similarity of the value, despite the different synthesis methods, suggests that Ta_3N_5 crystallinity is fundamentally compromised at oxygen contents above a few at.%.

An oxygen incorporation limit in Ta_3N_5 explains well the high temperatures and long process durations, i.e. a high thermal budget, necessary to obtain high crystallinity Ta_3N_5 by ammonolysis. The thermal budget is necessary to diffuse excess oxygen out of a Ta-O precursor and to substitute it by nitrogen. In magnetron sputtering, the oxygen-nitrogen substitution is not necessarily required due to the simultaneous incorporation of oxygen and nitrogen into the film. This allows a lower thermal budget for the onset of Ta_3N_5 crystallization with temperatures between 400° to 600° C applied only during the time of deposition [11].

Still, high substrate temperatures of up to 800° C are necessary to reach a high degree of crystallinity in experiments done by Ishihara *et al.* [11]. A possible explanation for this observation could be a high oxygen content in the films deposited at low substrate temperature. Similarly could the low crystallinity of magnetron-sputtered Ta_3N_5 samples prepared by Yokohama *et al.* [5] be explained by excess oxygen in the as-deposited films. Both Ishihara *et al.* [11] and Yokoyama *et al.* [5] use a total pressure similar to our study. However, in both studies, they use an O_2 partial pressure of 0.01 Pa, and between 0.013 and 0.07 Pa, respectively. These values are much higher by at least a factor of 3 compared to the 0.003 Pa used in our study for the most crystalline sample (deposited at 0.3 sccm O_2). In addition, the deposition rate in Yokoyama *et al.* is less than half our deposition rate (100 nm in 30 min [5] compared to 250 nm in 30 min in this study). As these films grow more slowly while being subjected to a higher O_2 partial pressure, they likely have a higher oxygen content compared to our most crystalline sample. Excess oxygen could thus explain the low crystallinity of their samples. In a similar way can our findings be used to explain improvements in crystallinity. Yokoyama *et al.* improve the crystallinity of their as-processed samples by a post-deposition annealing treatment in NH_3 [5]. This improved crystallinity can be attributed to a lower oxygen content in the films, as the samples are expected to lose oxygen during annealing. Ishihara *et al.* enhance the crystallinity by raising the substrate temperature which lowers the oxygen content in the films [11]. This is because a higher substrate temperature increases the reactivity of nitrogen which eases its incorporation into the growing film. As the oxygen supply to the growing film is limited, the oxygen/nitrogen ratio in the film is lowered. These examples show that our findings can explain changes in crystallinity of Ta_3N_5 thin films by variations of the oxygen content in the films.

The conclusion of this paper that oxygen determines the degree of crystallinity of Ta_3N_5 thin films can therefore also explain past observations on tuning the crystallinity of Ta_3N_5. The

observed correlation between the thermal budget and the sample crystallinity, however, is only an indirect one with the oxygen content in the film being the link between the two.

The fact that Ta_3N_5 tolerates only a limited amount of oxygen, has important implications for the application of this material as a photon absorber in solar water splitting devices. Many properties of Ta-O-N thin films can be tuned by varying the oxygen-to-nitrogen ratio, such as the band gap [6,33] and electronic properties [6]. However, if a Ta_3N_5 crystalline structure is desired, the range over which these properties can be tuned is limited. This applies especially to the position of the band edges that are important for achieving solar water splitting. The valence band edge of oxygen-free Ta_3N_5 is predicted to be too low with respect to the O_2/H_2O potential. Only with high oxygen doping, this band edge is sufficiently shifted [30] which may, however, not be compatible with a crystalline structure according to the findings of this paper.

4 Conclusion

This work identifies the oxygen content in Ta_3N_5 as the key parameter affecting the crystallinity of Ta_3N_5 thin films. A high level of oxygen incorporated into a film results in a low degree of crystallinity. This manifests in large amorphous regions into which few Ta_3N_5 crystallites are embedded. By lowering the oxygen supply during deposition, highly crystalline samples are obtained. This is possible by magnetron-sputtering as it allows a precise control of the oxygen incorporated homogeneously throughout the film thickness. The highest crystallinity is obtained for a sample containing 4.4 at.% of oxygen. This film exhibits large grains between 80 and 120 nm in size. The results show that the variations in degree of crystallinity of Ta_3N_5 thin films, observed by other authors, can largely be explained by different levels of oxygen incorporated into the material. This suggests a fundamental limit of oxygen incorporation before the crystallinity of Ta_3N_5 is compromised.

Acknowledgements

The authors thank the Centre National de la Recherche Scientifique (CNRS) for funding of this activity under grant agreement ANR-13-IS09-0003-01. The authors would like to thank Patrick Bonnaillie for the SEM images.

References

[1] W.-J. Chun, A. Ishikawa, H. Fujisawa, T. Takata, J. N. Kondo, M. Hara, M. Kawai, Y. Matsumoto, K. Domen, Conduction and valence band positions of Ta2O5, TaON, and Ta3N5 by UPS and electrochemical methods, J. Phys. Chem. B 107, 1798-1803, 2003.

[2] J. M. Morbec, I. Narkeviciute, T. F. Jaramillo, G. Galli, Optoelectronic properties of Ta_3N_5: A joint theoretical and experimental study, Phys. Rev. B 90, 155204, 2014.

[3] A.B. Murphy, P. R. F. Barnes, L. K. Randeniya, I. C. Plumb, I. E. Grey, M. D. Horne, J. A. Glasscock, Efficiency of solar water splitting using semiconductor electrods, Int. J. Hydrog. Energy 31, 1999-2017, 2006.

[4] M. Hara, E. Chiba, A. Ishikawa, T. Takata, J. N. Kondo, K. Domen, J. Phys. Chem. B 107, 13441-13445, 2003.

[5] D. Yokoyama, H. Hashiguchi, K. Maeda, T. Minegishi, T. Takata, R. Abe, J. Kubota, K. Domen, Ta3N5 photoanodes for water splitting prepared by sputtering, Thins Solid Films 519, 2087-2092, 2011.

[6] M. Rudolph, D. Stanescu, J. Alvarez, E. Foy, J.-P. Kleider, H. Magnan, T. Minea, H. Herlin-Boime, B. Bouchet-Fabre, M.-C. Hugon, The role of oxygen in magnetron-sputtered thin films of Ta_3N_5 for the photoelectrolysis of water, Surf. Coat. Technol. 324, 620-625, 2017.

[7] D. Lu, G. Hitoki, E. Katou, J. N. Kondo, M. Hara, K. Domen, Porous single-crystalline TaON and Ta3N5 particles, Chem. Mater. 16, 1603-1605, 2004.

[8] B. A. Pinaud, A. Vailionis, T. F. Jaramillo, Controlling the structural and optical properties of Ta3N5 films through nitridation temperature and the nature of the Ta metal, Chem. Mater 26, 1576-1582, 2014.

[9] A. Dabirian, R. van de Krol, Resonant optical absorption and defect control in Ta3N5 photoanodes, Appl. Phys. Lett. 102, 033905, 2013.

[10] S. J. Henderson, A. L. Hector, Structural and compositional variations in Ta3N5 produced by temperature amaonolysis of tantalum oxide, J. Sol. State Chem., 179, 3518-3524, 2006.

[11] A. Ishihara, S. Doi, S. Mitsushima, K.-I. Ota, Tantalum (oxy)nitrides prepared using reactive sputtering for new nonplatinum cathodes of polymer electrolyte fuel cell, Electrochim. Acta 53, 5442-5450, 2008.

[12] M. Rudolph, A. Demeter, E. Foy, V. Tiron, L. Sirghi, T. Minea, B. Bouchet-Fabre, M.-C. Hugon, Improving the degree of crystallinity of magnetron-sputtered Ta3N5 thin films by augmenting the ion flux onto the substrate, Thin Solid Films, 636, 48-53, 2017.

[13] M. Rudolph, D. Lundin, E. Foy, M. Debognie, M.-C. Hugon, T. Minea, Influence of backscattered neutrals on the grain size of magnetron-sputtered TaN thin films, Thin Solid Films 658, 46-53, 2018.

[14] A. P. Hammersley, FIT2D: a multi-purpose data reduction, analysis and visualization program, J. Appl. Cryst. 49, 646-652, 2016.

[15] Rioult M., Magnan H., Stanescu D., Barbier A., Single Crystalline Hematite films for Solar Water Splitting: Ti Doping and Thickness Effects, J. Phys. Chem. C, 118, 3007–3014, 2014.

[16] X. Sun, E. Kolawa, J.-S. Chen, J. S. Reid, M-A. Nicolet, Properties of reactively sputter-deposited Ta-N thin films, Thin Solid Films, 236, 1-2, 347-351, 1993.

[17] A. Fuertes, Synthesis and properties of functional oxynitrides – from photocatalysts to CMR materials, Dalton Trans. 39, 5942 -5948, 2010.

[18] S. Berg, T. Nyberg, Fundamental understanding and modeling of reactive sputtering processes, Thin Solid Films 476, 215-230, 2005.

[19] N. Terao, Structure of tantalum nitrides, Jpn. J. Appl. Phys. 10, 2, 248-259, 1971.

[20] J. Strähle, Die Kristallstruktur des Tantal(V)-nitrids Ta_3N_5, Z. Anorg. Allg. Chem. 402, 47-57, 1973.

[21] N. E. Brese, M. O'Keefe, P. Rauch, F. J. Disalvo, Structure of Ta_3N_5 at 16 K by time-of-flight neutron diffraction, Acta Cryst. C47, 2291-2294, 1991.

[22] M. Stavrev, D. Fischer, C. Wenzel, K. Drescher, N. Mattern, Crystallographic and morphological characterization of reactively sputtered Ta, Ta-N and Ta-N-O thin films, Thin Solid Films 307, no. 1-2, 79 – 88, 1997.

[23] A. Bousquet, F. Zoubian, J. Cellier, C. Taviot-Gueho, T. Sauvage, E. Tomasella, Structural and ellipsometric study on tailored optical properties of tantalum oxynitride films deposited by reactive sputtering, J. Phys. D: Appl. Phys. 47, 475201, 2014.

[24] K. Holloway, P. M. Fryer, Tantalum as a diffusion barrier between copper and silicon, Appl. Phys. Lett. 57, 1736-1738, 1990.

[25] M. de Respinis, M. Fravventura, F. F. Abdi, H. Schreuders, T. J. Savenije, W. A. Smith, B. Dam, R. van de Krol, Oxynitrogenography : Controlled synthesis of single-phase tantalum oxynitride photoabsorbers, Chem. Mater. 27, 7091-7099, 2015.

[26] A. Ishikawa, T. Takata, J. N. Kondo, M. Hara, K. Domen, Electrochemical behavior of thin Ta3N5 semiconductor film, J. Phys. Chem. B 108, 11049 – 11053, 2004.

[27] Y. He, J. Thorne, C. Hao Wu, P. Ma, C. Du, Q. Dong, J. Guo, , D. Wang, What limits the performace of Ta3N5 for solar water splitting?, Chem 1, 640-655, 2016.

[28] Y. Li, L. Zhang, A. Torre-Pardo, J. M. Gonzáles-Calbet, Y. Ma, P. Oleynikov, O. Terasaki, S. Asahina, M. Shima, D. Cha, L. Zhao, K. Takanabe, J. Kubota, K. Domen, Cobalt-Phosphate-modified barium-doped tantalum nitride nanorod photoanode with 1.5% solar energy conversion efficiency, Nat. Commun. 4:2566, 2013.

[29] K. Maeda, K. Domen, New non-oxide photocatalysts designed for overall water splitting under visible light, J. Phys. Chem. C 111, 7851-7861, 2007.

[30] M. Harb, P. Sautet, E. Nurlaela, P. Raybaud, L. Cavallo, K. Domen, J.-M. Basset, K. Takanabe, Tuning the properties of visible-light-responsive tantalum (oxy)nitride photocatalysts by non-stoichiometric compositions: a first-principles viewpoint, Phys. Chem. Chem. Phys. 16, 20548-20560, 2014.

[31] Y. Li, T. Takata, D. Cha, K. Takanabe, T. Minegishi, J. Kubota, K. Domen, Vertically aligned Ta3N5 nanorod arrays for solar-driven photoelectrochemical water splitting, Adv. Mater. 25, 125-131, 2013.

[32] S. Mráz, J. M. Schneider, Influence of the negative oxygen ions on the structure evolution of transition metal oxide thin films, J. Appl. Phys. 100, 023503, 2006.

[33] A. Bousquet, F. Zoubian, J. Cellier, C. Tavio-Gueho, T. Sauvage, E. Tomasella, Structural and ellipsomtetric strudy on tailored optical properties of tantalum oxynitride films deposited by reactive sputtering, J. Phys. D Appl. Phys. 47, 475201, 2014.